Boundary conditions for the electron wavefunction in GaInNAs-based quantum wells and modelling of the temperature-dependent bandgap

2004 J. Phys.: Condens. Matter 16 S3151

(http://iopscience.iop.org/0953-8984/16/31/011)

INSTITUTE OF PHYSICS PUBLISHING JOURNAL OF PHYSICS: CONDENSED MATTER

J. Phys.: Condens. Matter **16** (2004) S3151–S3159 PII: S0953-8984(04)74048-5

Boundary conditions for the electron wavefunction in GaInNAs-based quantum wells and modelling of the temperature-dependent bandgap

M Hetterich[1,3], A Grau[1], A Yu Egorov[2] and H Riechert[2]

[1] Institut für Angewandte Physik and Center for Functional Nanostructures (CFN), Universität Karlsruhe (TH), 76131 Karlsruhe, Germany
[2] Infineon Technologies, 81730 München, Germany

E-mail: michael.hetterich@physik.uni-karlsruhe.de

Received 31 December 2003
Published 23 July 2004
Online at stacks.iop.org/JPhysCM/16/S3151
doi:10.1088/0953-8984/16/31/011

Abstract

In this paper we derive and discuss the boundary conditions for the electron wavefunction in general $Ga_{1-x}In_xN_yAs_{1-y}$-based heterostructures described by the band anticrossing model. The use of these boundary conditions greatly simplifies the calculation of, for example, transition energies in quantum wells. We then apply the derived equations to model the temperature-dependent bandgap of $Ga_{1-x}In_xN_yAs_{1-y}$/GaAs quantum well structures with high indium concentrations. From a fit to our experimental photoreflectance data we find evidence that the effective nitrogen level E_N in the band anticrossing Hamiltonian, measured with respect to the valence band edge, shifts to higher energies with decreasing temperature. This supports and extends similar results reported in the literature for low indium content epilayers.

1. Introduction

In recent years, $Ga_{1-x}In_xN_yAs_{1-y}$ has attracted considerable interest as a promising material for the realization of optoelectronic devices operating at telecom wavelengths in the near-infrared. From a band structure point of view, the properties of this quaternary alloy are quite unusual: incorporation of only a few per cent of nitrogen into Ga(In)As leads to a strong bandgap reduction, the appearance of the so-called E_+ band above the band edge, an increased effective electron mass and a significant conduction band nonparabolicity [1–7]. In the so-called band anticrossing (BAC) model [4] these effects are interpreted to be the result of a

[3] Author to whom any correspondence should be addressed.

repulsive interaction between the conduction band and a (strongly localized) nitrogen-related energy level E_N above the conduction band edge. For bulk material the model Hamiltonian is

$$\begin{pmatrix} E_M(\boldsymbol{k}) & V_{NM} \\ V_{NM} & E_N \end{pmatrix} \tag{1}$$

where $E_M(\boldsymbol{k})$ is the conduction band dispersion of the host $Ga_{1-x}In_xAs$ matrix M and V_{NM} represents the coupling of the latter with the nitrogen level. By solving the characteristic equation

$$\begin{vmatrix} E_M(\boldsymbol{k}) - E & V_{NM} \\ V_{NM} & E_N - E \end{vmatrix} = 0 \tag{2}$$

one obtains the $\boldsymbol{k}$-dependent eigenvalues of (1), which correspond to the experimentally observed upper $E_+(\boldsymbol{k})$ and lower $E_-(\boldsymbol{k})$ ($Ga_{1-x}In_xN_yAs_{1-y}$ conduction band) states. V_{NM} depends on the nitrogen concentration y as [4, 7]

$$V_{NM} = C_{NM}\sqrt{y}, \tag{3}$$

where C_{NM} is a constant coupling parameter. It has also been pointed out in [7] that E_N and E_M are themselves y-dependent. Therefore, $E_M(\boldsymbol{k})$ actually represents the conduction band dispersion of $Ga_{1-x}In_xN_yAs_{1-y}$, neglecting the interaction with E_N.

It is actually quite nontrivial that an approach as simple as the model just presented should be able to describe the complex effects of nitrogen on the $Ga_{1-x}In_xN_yAs_{1-y}$ band structure. Indeed, the results of empirical pseudopotential calculations [8] suggest that the observed anticrossing in GaN_yAs_{1-y} can, in general, not be ascribed to the interaction of the conduction band with a single nitrogen level. The incorporation of nitrogen into GaAs removes the translational symmetry of the crystal, thus splitting, for example, the L_{1c} valleys into $a_1(L_{1c}) + t_2(L_{1c})$ states and X_{1c} into $a_1(X_{1c}) + e(X_{1c})$. The conduction band valley Γ_{1c} remains as $a_1(\Gamma_{1c})$. Higher-energy host crystal bands are also perturbed, producing, among others, a_1 states of their own. In particular, in the dilute nitrogen regime, an additional nitrogen localized state built from many high-energy host bands forms above the conduction band minimum of GaAs. However, *all* states of the same symmetry representation can be expected to interact under the perturbation due to the presence of N, i.e. we should have a coupling and anticrossing of *all* a_1-like states (Γ, X, L band edges, etc) instead of the two-level BAC approach where only the interaction of the conduction band with the localized nitrogen level E_N is taken into account. Applying the BAC model therefore actually means that we replace the complex interaction with higher energy states by the coupling to only *one* 'effective' nitrogen level E_N (which, in general, may not correspond to a real state) to get a simple description of the Ga(In)NAs band structure. Indeed, there is some theoretical support for this initially semi-empirical approach: using a Green function model it has been shown that the two-level BAC model (with an 'effective' E_N) can be derived explicitly, if only the influence of the onsite change in orbital energies due to the N impurity is considered [9]. In further numerical calculations the authors also find evidence that the model should stay appropriate when treating the full Hamiltonian.

From an experimental point of view this result is confirmed by the fact that the BAC model has been applied very successfully so far. It has proven its ability to accurately describe not only the electronic states in bulk material but also in quantum well (QW) structures many times and can therefore be regarded as well established (see, e.g., [1–5, 10–14] and references therein). However, the technologically important calculation of quantum well states usually requires a numerical diagonalization of the BAC Hamiltonian. In the following we suggest a different, much simpler approach which circumvents this cumbersome procedure. The latter takes advantage of the special boundary conditions for the electron wavefunction in

$Ga_{1-x}In_xN_yAs_{1-y}$ heterostructures and is discussed in the next two sections. Then we proceed with a first typical application of the described calculation technique, namely the theoretical modelling of the temperature-dependent effective bandgap in $Ga_{1-x}In_xN_yAs_{1-y}$/GaAs QW structures. In particular we present evidence from a fit to our experimental photoreflectance (PR) data that the effective nitrogen level E_N in the BAC Hamiltonian, measured with respect to the valence band edge, shifts to higher energies with decreasing temperature.

2. Boundary conditions for the BAC model wavefunction in GaInNAs-based heterostructures

When the band anticrossing model is applied to a quantum well or any other structure with a spatially varying composition profile along the growth direction z, all material parameters in the BAC Hamiltonian become position-dependent. Furthermore, $E_M(\boldsymbol{k})$ has to be replaced by a suitable Hermitian operator. For the latter we choose

$$E_M(z) - \frac{\hbar^2}{2}\frac{\partial}{\partial z}\frac{1}{m^*(z)}\frac{\partial}{\partial z} \tag{4}$$

which has already been used quite successfully in the past also for quantum structures based on $Ga_{1-x}In_xN_yAs_{1-y}$ [10]. $E_M(z)$ and $m^*(z)$ are the z-dependent conduction band edge and effective mass, respectively, that would be obtained if no anticrossing with E_N was present. In practice, their values should essentially coincide with those of the corresponding nitrogen-free material. The kinetic energy operator chosen in (4) implies that we assume a parabolic dispersion for the unperturbed conduction band of the matrix material. For the E_- branch ($Ga_{1-x}In_xN_yAs_{1-y}$ conduction band) which we are primarily interested in, this approximation is, in our experience, usually sufficient, because a nonparabolicity in $E_M(\boldsymbol{k})$ would occur for high k values where $E_-(\boldsymbol{k})$ flattens out anyway due to the strong anticrossing with the nitrogen level. With the changes just discussed the total BAC Hamiltonian for the one-dimensional case is now

$$H^{BAC} = \begin{pmatrix} E_M(z) - \frac{\hbar^2}{2}\frac{\partial}{\partial z}\frac{1}{m^*(z)}\frac{\partial}{\partial z} & V_{NM}(z) \\ V_{NM}(z) & E_N(z) \end{pmatrix} \tag{5}$$

and the corresponding time-dependent Schrödinger equation becomes

$$H^{BAC}\begin{pmatrix} \Psi_M(z,t) \\ \Psi_N(z,t) \end{pmatrix} = i\hbar\frac{\partial}{\partial t}\begin{pmatrix} \Psi_M(z,t) \\ \Psi_N(z,t) \end{pmatrix}. \tag{6}$$

Let us now turn to the probability current density $j(z,t)$ of the BAC model. The latter can be deduced by calculating the time derivative of the probability density:

$$\rho(z,t) = \Psi_M(z,t)\Psi_M^*(z,t) + \Psi_N(z,t)\Psi_N^*(z,t) \tag{7}$$

using (6). After some mathematics one finally obtains the continuity equation

$$\frac{\partial\rho(z,t)}{\partial t} + \frac{\partial j(z,t)}{\partial z} = 0 \tag{8}$$

with the probability current density

$$j(z,t) = \frac{1}{2m^*(z)}\left[\Psi_M^*(z,t)\frac{\hbar}{i}\frac{\partial}{\partial z}\Psi_M(z,t) - \Psi_M(z,t)\frac{\hbar}{i}\frac{\partial}{\partial z}\Psi_M^*(z,t)\right]. \tag{9}$$

It is interesting to note that there is no contribution of $\Psi_N(z,t)$ to j. This is caused by the fact that E_N is dispersionless and reflects the localized nature of the nitrogen states.

Based on the equations presented so far we are now able to investigate the boundary conditions for the solutions of the stationary Schrödinger equation

$$H^{\mathrm{BAC}} \begin{pmatrix} \psi_{\mathrm{M}}(z) \\ \psi_{\mathrm{N}}(z) \end{pmatrix} = E \begin{pmatrix} \psi_{\mathrm{M}}(z) \\ \psi_{\mathrm{N}}(z) \end{pmatrix} \tag{10}$$

at the interface between two homogeneous $Ga_{1-x}In_xN_yAs_{1-y}$ layers A and B with different compositions. The first point to make here is that the lower component $\psi_{\mathrm{N}}(z)$ of the wavefunction is, in general, *discontinuous* at the interface. Let us first discuss this for the (somewhat unphysical) special case $V_{\mathrm{NM}}(z) = 0$: from the Schrödinger equation (10) we obtain $E_{\mathrm{N}}(z)\psi_{\mathrm{N}}(z) = E\psi_{\mathrm{N}}(z)$. This equation only leads to a nonvanishing $\psi_{\mathrm{N}}(z)$ if

$$E = E_{\mathrm{N}}(z). \tag{11}$$

For a single homogeneous $Ga_{1-x}In_xN_yAs_{1-y}$ layer we would have $E_{\mathrm{N}}(z) = E_{\mathrm{N}}$. Therefore, all nitrogen-like eigenfunctions would correspond to the same eigenvalue:

$$E = E_{\mathrm{N}}, \tag{12}$$

as expected. However, the eigenfunctions themselves could have arbitrary shape. This is related to the fact already mentioned above that there is no contribution of the nitrogen states to the probability current density. As a consequence the values of $\psi_{\mathrm{N}}(z)$ at different positions are completely decoupled and will always result in a stationary solution of the Schrödinger equation. (This changes for $V_{\mathrm{NM}} \neq 0$, because different sites become indirectly coupled via the E_{M} states.)

If we now repeat the procedure described in the last paragraph for the case of two interfacing layers A and B, (12) holds for both sides of the interface separately, i.e. there are states with $E = E_{\mathrm{N}}^{\mathrm{A}}$ and $E = E_{\mathrm{N}}^{\mathrm{B}}$, respectively. Since the energetic position of E_{N} depends on both the composition and microscopic structure of the layer under consideration (see, e.g., [13]), we will generally have $E_{\mathrm{N}}^{\mathrm{A}} \neq E_{\mathrm{N}}^{\mathrm{B}}$. For that reason, (11) can only be satisfied on both sides simultaneously, if $\psi_{\mathrm{N}}(z)$ vanishes identically in material B for states with $E = E_{\mathrm{N}}^{\mathrm{A}}$ and vice versa. In other words, each type of nitrogen wavefunction is confined to its own material (where it can have arbitrary shape, see above). However, this implies that $\psi_{\mathrm{N}}(z)$ is, in general, *discontinuous* at the interface.

For the realistic case $V_{\mathrm{NM}} \neq 0$ the situation becomes more complicated. From the Schrödinger equation (10) we now obtain

$$\psi_{\mathrm{N}}(z) = \frac{V_{\mathrm{NM}}(z)}{E - E_{\mathrm{N}}(z)} \psi_{\mathrm{M}}(z), \tag{13}$$

i.e. $\psi_{\mathrm{N}}(z)$ and $\psi_{\mathrm{M}}(z)$ become coupled. As shown below, $\psi_{\mathrm{M}}(z)$ is continuous at the interface. However, $V_{\mathrm{NM}}(z)$ and $E_{\mathrm{N}}(z)$ are of course both discontinuous, which means $\psi_{\mathrm{N}}(z)$ cannot be continuous for all possible energy values E either.

Let us now proceed with the more important boundary conditions for the upper component $\psi_{\mathrm{M}}(z)$ of the BAC wavefunction. For a heterostructure containing two $Ga_{1-x}In_xN_yAs_{1-y}$ layers with different compositions interfacing at $z = 0$ we integrate (10) over an infinitesimal interval $[-\varepsilon, +\varepsilon]$:

$$\int_{-\varepsilon}^{+\varepsilon} \left\{ E_{\mathrm{M}}(z)\psi_{\mathrm{M}}(z) - \frac{\hbar^2}{2} \frac{\partial}{\partial z} \left[\frac{1}{m^*(z)} \frac{\partial}{\partial z} \psi_{\mathrm{M}}(z) \right] + V_{\mathrm{NM}}(z)\psi_{\mathrm{N}}(z) \right\} \mathrm{d}z = E \int_{-\varepsilon}^{+\varepsilon} \psi_{\mathrm{M}}(z)\, \mathrm{d}z. \tag{14}$$

In the limit $\varepsilon \to 0$ all terms apart from the second vanish. Carrying out the integration therefore finally leads to the boundary condition

$$\frac{1}{m^*(-\varepsilon)} \frac{\partial}{\partial z} \psi_{\mathrm{M}}(-\varepsilon) = \frac{1}{m^*(+\varepsilon)} \frac{\partial}{\partial z} \psi_{\mathrm{M}}(+\varepsilon), \tag{15}$$

which means $\psi'_{\mathrm{M}}(z)/m^*(z)$ has to be continuous at the interface. This expression looks very similar to the commonly used condition for quantum wells with different effective masses in the well and barrier material, respectively (see, e.g., [15]). However, the important difference to note is that, for nitrogen-containing material, m^* does *not* correspond to the actual effective electron mass itself but rather to the value that would be obtained if there was no anticrossing interaction of E_{M} with E_{N}. In other words, m^* is essentially the effective mass of the $\mathrm{Ga}_{1-x}\mathrm{In}_x\mathrm{As}$ matrix.

The second boundary condition for $\psi_{\mathrm{M}}(z)$ follows from the continuity equation (8). For the stationary case $\partial\rho/\partial t = 0$ the latter implies that the probability current density $j(z)$ is the same at both sides of the interface. Using (9) and (15) it follows that for $\varepsilon \to 0$

$$\psi_{\mathrm{M}}(-\varepsilon) = \psi_{\mathrm{M}}(+\varepsilon) \tag{16}$$

i.e. $\psi_{\mathrm{M}}(z)$ must be continuous at the interface.

3. BAC model calculation of bound states in GaInNAs quantum wells

Based on the derived boundary conditions (15) and (16) we can now quite easily calculate the E_-- and E_+-related bound states in $\mathrm{Ga}_{1-x}\mathrm{In}_x\mathrm{N}_y\mathrm{As}_{1-y}$-based quantum well structures. It is interesting to note that this is possible without explicitly treating $\psi_{\mathrm{N}}(z)$, since neither (15) nor (16) contains this component of the wavefunction. We start by using (13) to eliminate $\psi_{\mathrm{N}}(z)$ from the Schrödinger equation (10). One obtains

$$-\frac{\hbar^2}{2}\frac{\partial}{\partial z}\frac{1}{m^*(z)}\frac{\partial}{\partial z}\psi_{\mathrm{M}}(z) + \left[E_{\mathrm{M}}(z) + \frac{V_{\mathrm{NM}}^2(z)}{E - E_{\mathrm{N}}(z)}\right]\psi_{\mathrm{M}}(z) = E\psi_{\mathrm{M}}(z). \tag{17}$$

This is the ordinary Schrödinger equation for systems with a position-dependent effective mass [15], apart from an additional energy-dependent contribution $V_{\mathrm{NM}}^2(z)/[E - E_{\mathrm{N}}(z)]$ to the potential energy caused by the interaction with the nitrogen states. Equation (17) can be solved using the standard ansatz

$$\psi_{\mathrm{M}}(z) = \begin{cases} A\exp(\mathrm{i}kz) + B\exp(-\mathrm{i}kz) & \text{(well)} \\ C\exp(\kappa z) + D\exp(-\kappa z) & \text{(barrier)} \end{cases} \tag{18}$$

which leads to

$$\begin{aligned} k &= \left\{\frac{2m^*(\mathrm{A})}{\hbar^2}\left[E - E_{\mathrm{M}}(\mathrm{A}) + \frac{V_{\mathrm{NM}}^2(\mathrm{A})}{E_{\mathrm{N}}(\mathrm{A}) - E}\right]\right\}^{\frac{1}{2}} \qquad \text{(well material A)} \\ \kappa &= \left\{\frac{2m^*(\mathrm{B})}{\hbar^2}\left[E_{\mathrm{M}}(\mathrm{B}) - E - \frac{V_{\mathrm{NM}}^2(\mathrm{B})}{E_{\mathrm{N}}(\mathrm{B}) - E}\right]\right\}^{\frac{1}{2}} \qquad \text{(barrier material B).} \end{aligned} \tag{19}$$

The latter equations clearly reflect the strongly nonparabolic dispersion of the $\mathrm{Ga}_{1-x}\mathrm{In}_x\mathrm{N}_y\mathrm{As}_{1-y}$ conduction band near the nitrogen level E_{N}. This nonparabolicity leads to a significant deviation of the quantization energies for E_--derived states with high k (e.g. excited conduction band states) in comparison to a simple effective mass model. Only for E_- states with small k the dispersion relation becomes approximately parabolic. The quantization energies obtained for this case are therefore similar to those that would be obtained from a simplified single-band effective mass model, taking into account the modified conduction band mass due to the BAC interaction. However, it is important to note that, even for states with small k, the results of both procedures are not *exactly* the same because they correspond to slightly different boundary conditions, in particular for the derivative of the wavefunction (see (15)).

Since the Schrödinger equation (17) as well as the boundary conditions (15) and (16) for $\psi_{\mathrm{M}}(z)$ in the BAC model are formally identical to those of the textbook quantum well (apart from the additional contribution to the potential energy, the different meaning of m^* and the changed dispersion relation) the energies of the bound eigenstates can be found by numerically solving the well-known implicit equations [15]:

$$\begin{aligned} &\cos\left(\frac{1}{2}kL\right) - \frac{m^*(\mathrm{B})k}{m^*(\mathrm{A})\kappa}\sin\left(\frac{1}{2}kL\right) = 0 \qquad \text{(even states)} \\ &\cos\left(\frac{1}{2}kL\right) + \frac{m^*(\mathrm{A})\kappa}{m^*(\mathrm{B})k}\sin\left(\frac{1}{2}kL\right) = 0 \qquad \text{(odd states)} \end{aligned} \tag{20}$$

where L is the thickness of the quantum well. In practice, E is scanned from the bottom to the top of the quantum well (in the energy range of the E_- and E_+ branches), k and κ are calculated for each E using (19) and the energy eigenvalues are then found by checking if one of equations (20) is satisfied.

The described procedure is much simpler, faster and more transparent than the usual numerical diagonalization of the BAC Hamiltonian and therefore ideally suited for the fitting of experimental data. In the next section, we describe an example for the successful application of this approach, namely the theoretical modelling of the temperature-dependent effective bandgap in $Ga_{1-x}In_xN_yAs_{1-y}$/GaAs multiple quantum wells (MQWs) measured by photoreflectance spectroscopy.

4. Temperature dependence of the effective bandgap in GaInNAs/GaAs multiple quantum wells

It is well known that the incorporation of nitrogen into Ga(In)As quantum wells or bulk material leads to a reduced temperature dependence of the bandgap. Within the BAC model this quenching effect can be interpreted as a consequence of the repulsive interaction between the host conduction band E_{M} and the nitrogen level E_{N} (see, e.g., [2, 3, 11, 12, 14]). However, for a quantitative modelling of the thermally induced bandgap variation we need to know the temperature dependence of E_{N}. This is particularly crucial in quantum well structures, where the effective bandgap is defined by the lowest possible transition energy between quantized electron and hole states (in our case the e1–hh1 heavy hole transition). Here the energetic position of the nitrogen level influences not only the bandgap of the material itself but also the conduction band dispersion and therefore the quantization energies. Unfortunately, little is known about $E_{\mathrm{N}}(T)$ up to now, although recent investigations seem to indicate a shift to higher energies relative to the valence band edge with decreasing temperature [2, 3].

In this paper we present some of our results concerning the temperature dependence of the e1–hh1 transition in GaInNAs/GaAs MQWs measured by photoreflectance spectroscopy. The electronic structure at room temperature for the particular sample discussed below has already been investigated in detail before [10]. This provides us with an ideal basis for the modelling of the present temperature-dependent data from which some information about the thermal shift of E_{N} can be extracted.

4.1. Experimental details

The GaInNAs/GaAs MQW structures discussed here were grown by solid-source molecular-beam epitaxy on GaAs(001) using a RF-coupled plasma source for nitrogen. Afterwards they were annealed at about 750 °C, where the resulting blue-shift in photoluminescence [1] saturates (in good agreement with the results described in [13]). For the PR measurements

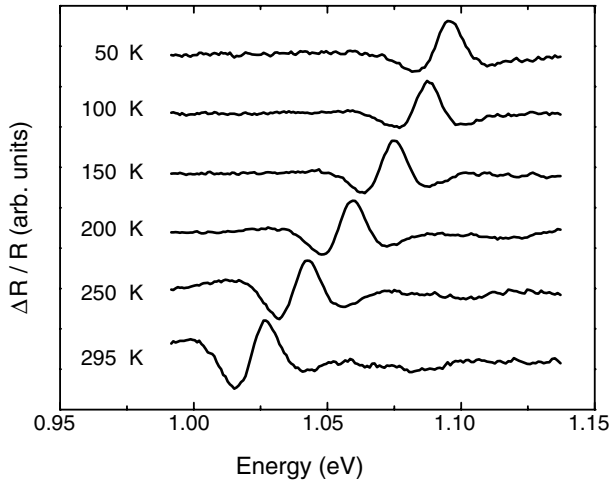

Figure 1. Temperature-dependent PR spectra of a $Ga_{0.7}In_{0.3}N_{0.017}As_{0.983}$/GaAs MQW with 6.2 nm well width. For clarity, the spectra are shifted vertically relative to each other and have different scaling factors.

we used a standard set-up in which a 670 nm laser diode followed by a chopper provided the photomodulation. Mounting the samples in a cryostat enabled us to perform the temperature-dependent experiments between 50 and 295 K described in the next section.

4.2. Results and discussion

Figure 1 shows the measured temperature-dependent PR spectra for a sample containing five $Ga_{0.7}In_{0.3}N_{0.017}As_{0.983}$ quantum wells with 6.2 nm well widths and GaAs barriers. A clear resonance due to the lowest e1–hh1 transition is observed in all cases. As expected, the latter shifts to lower energies with increasing temperature, indicating a decreasing bandgap. To extract accurate transition energy values from the measured PR spectra, fits based on the first derivative functional form, assuming a Gaussian lineshape for the dielectric function [16], have been used. Since weaker, partly unresolved higher energy transitions also contribute to the PR signal we have taken them into account in our fit where necessary, particularly for the spectra taken at elevated temperatures (see [10] for further details). The values obtained for the temperature dependence of the e1–hh1 transition in this way are shown as data points in figure 2.

In order to analyse these experimental results within the BAC model, a computer program based on the equations in section 3 has been developed. All GaAs and GaInAs material parameters entering the program have been chosen according to [17]. The temperature dependence of the bandgaps is obtained from the Varshni equation [18] and the corresponding change in the effective masses can then be derived by applying $\boldsymbol{k}\cdot\boldsymbol{p}$ theory (see, e.g., [17]). We have also included the influence of (temperature-dependent) strain on the electronic structure of the $Ga_{1-x}In_xAs$ matrix, however, excitonic effects are neglected. The $Ga_{1-x}In_xN_yAs_{1-y}$-specific material parameters at room temperature have been adopted from our previous studies [10]. In the latter a series of annealed MQWs with varying In concentration (including the one discussed here) was investigated by PR. From a theoretical fit to the whole set of electronic transitions observed in the room-temperature spectra we found that C_{NM}, the parameter in the hybridization matrix element, decreases significantly when the

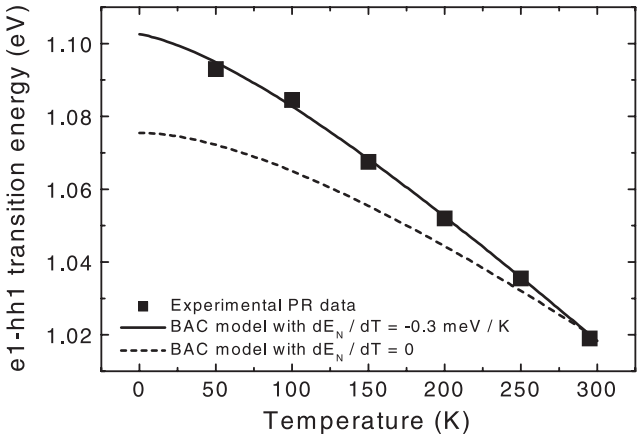

Figure 2. Temperature dependence of the e1–hh1 transition energy in a $Ga_{0.7}In_{0.3}N_{0.017}As_{0.983}$/GaAs MQW with 6.2 nm well width. The experimental data points have been extracted from PR measurements, while the full and broken curves are theoretical predictions of the BAC model assuming $dE_N/dT = -0.3$ meV K^{-1} and $dE_N/dT = 0$, respectively.

In concentration in $Ga_{1-x}In_xN_yAs_{1-y}$ increases. For the case of $x = 0.3$ discussed here, $C_{NM} = 1.75$ eV. Following [2, 3] we assume this value to be temperature-independent in our present calculations. It should be noted that the same assumption is also made for the absolute unstrained valence band offset. However, the choice of the latter is quite uncritical for the predictions of our model anyway.

Based on the computational approach described above we are now able to extract the temperature dependence of the nitrogen level E_N—measured with respect to the (itself temperature-dependent) valence band edge—from a fit to our experimental PR data. The broken curve in figure 2 shows the expected thermal shift of the e1–hh1 transition, according to the BAC model, if we assume E_N to be temperature-independent and fixed to its room-temperature value. Obviously, the calculated shift is significantly smaller than that found in experiment. On the other hand, excellent agreement between measurement and theory is found for a nitrogen-free test sample with similar In concentration. We believe this to indicate that the nitrogen level cannot be—as often assumed—temperature-independent. Instead, E_N is suggested to move to higher energies with decreasing temperature, thus decreasing the anticrossing-induced quenching of the thermal effective bandgap shift. Indeed, we find good agreement of the BAC model prediction with our experimental data, if we assume a linear dependence for $E_N(T)$ with $dE_N/dT = -0.3$ meV K^{-1} (full curve in figure 2). It should also be mentioned that preliminary investigations of additional samples with lower In concentrations yield very similar values. This supports and extends the results recently reported in [2, 3], where the authors obtained $dE_N/dT = -0.25$ meV K^{-1} from absorption measurements on free-standing $Ga_{0.93}In_{0.07}N_{0.004}As_{0.996}$ and $Ga_{0.96}In_{0.04}N_{0.01}As_{0.99}$ layers.

5. Summary and conclusions

In the theoretical part of this paper we have derived and discussed the boundary conditions for the electron wavefunction in $Ga_{1-x}In_xN_yAs_{1-y}$-based heterostructures described within the band anticrossing model. Based on these equations a procedure for the calculation of quantum well states could be developed which avoids the cumbersome numerical diagonalization of the

BAC Hamiltonian. In the experimental part of the paper this approach has then been applied to model the temperature dependence of the e1–hh1 transition in $Ga_{1-x}In_xN_yAs_{1-y}$/GaAs quantum well structures measured by PR. From fits to our experimental data we find evidence that the nitrogen level E_N in $Ga_{1-x}In_xN_yAs_{1-y}$, measured with respect to the valence band edge, shifts to higher energies with decreasing temperature. This supports and extends similar results reported in the literature for low indium content epilayers.

Acknowledgments

This work has been financially supported by the Deutsche Forschungsgemeinschaft (DFG) within the Emmy Noether programme and the Center for Functional Nanostructures (CFN) at the University of Karlsruhe (project A2.2).

References

[1] Buyanova I A, Chen W M and Monemar B 2001 *MRS Internet J. Nitride Semicond. Res.* **6** 2
[2] Skierbiszewski C, Perlin P, Wisniewski P, Suski T, Geisz J F, Hingerl K, Jantsch W, Mars D E and Walukiewicz W 2001 *Phys. Rev.* B **65** 035207
[3] Skierbiszewski C 2002 *Semicond. Sci. Technol.* **17** 803
[4] Shan W, Walukiewicz W, Yu K M, Ager J W III, Haller E E, Geisz J F, Friedman D J, Olson J M, Kurtz S R, Xin H P and Tu C W 2001 *Phys. Status Solidi* b **223** 75
[5] Klar P J, Grüning H, Heimbrodt W, Weiser G, Koch J, Volz K, Stolz W, Koch S W, Tomić S, Choulis S A, Hosea T J C, O'Reilly E P, Hofmann M, Hader J and Moloney J V 2002 *Semicond. Sci. Technol.* **17** 830
[6] Hetterich M, Dawson M D, Egorov A Yu, Bernklau D and Riechert H 2000 *Appl. Phys. Lett.* **76** 1030
[7] Lindsay A and O'Reilly E P 1999 *Solid State Commun.* **112** 443
[8] Kent P R C and Zunger A 2001 *Phys. Rev.* B **64** 115208
[9] O'Reilly E P, Lindsay A, Tomić S and Kamal-Saadi M 2002 *Semicond. Sci. Technol.* **17** 870
[10] Hetterich M, Grau A, Egorov A Yu and Riechert H 2003 *J. Appl. Phys.* **94** 1810
[11] Suemune I, Uesugi K and Walukiewicz W 2000 *Appl. Phys. Lett.* **77** 3021
[12] Potter R J, Balkan N, Marie X, Carrère H, Bedel E and Lacoste G 2001 *Phys. Status Solidi* a **187** 623
[13] Klar P J, Grüning H, Koch J, Schäfer S, Volz K, Stolz W, Heimbrodt W, Kamal Saadi A M, Lindsay A and O'Reilly E P 2001 *Phys. Rev.* B **64** 121203(R)
[14] Polimeni A, Capizzi M, Geddo M, Fischer M, Reinhardt M and Forchel A 2001 *Phys. Rev.* B **63** 195320
[15] Bastard G 1988 *Wave Mechanics Applied to Semiconductor Heterostructures* (Les Ulis: Les Editions de Physique) pp 74–76, 112 and 113
[16] Pollak F H 1994 *Handbook on Semiconductors* vol 2, ed M Balkanski (Amsterdam: North-Holland) p 527
[17] Vurgaftman I, Meyer J R and Ram-Mohan L R 2001 *J. Appl. Phys.* **89** 5815
[18] Varshni Y P 1967 *Physica* **34** 149